The Physics of Electron Internal Transport Barriers in the TCV Tokamak

S. Coda, E. Asp, E. Fable, T.P. Goodman, O. Sauter, V.S. Udintsev, R. Behn, M.A. Henderson, A. Marinoni, G.P. Turri, C. Zucca, and the TCV team

Ecole Polytechnique Fédérale de Lausanne, Centre de Recherches en Physique des Plasmas, Association EURATOM-Confédération Suisse, EPFL SB CRPP, Station 13, CH-1015 Lausanne, Switzerland

e-mail contact of main author: stefano.coda@epfl.ch

Abstract - Electron internal transport barriers (eITBs) are generated in the TCV tokamak with strong electron cyclotron resonance heating (ECRH) in a variety of conditions, ranging from steady-state fully non-inductive scenarios to stationary discharges with a finite inductive component, and finally to transient current ramps without current drive. The confinement improvement over L-mode ranges from 3 to 6; the bootstrap current fraction is invariably large and is above 70% in the highest confinement cases, with good current-profile alignment permitting the attainment of steady state. Barriers are observed both in the electron temperature and density profiles, with a strong correlation both in location and in steepness. The dominant role of the current profile in the formation and properties of eITBs has been conclusively proven in a TCV experiment exploiting the large current-drive efficiency of the Ohmic transformer: small current perturbations accompanied by negligible energy transfer dramatically alter the confinement. The crucial element in the formation of the barrier is the appearance of a central region of negative magnetic shear, with the barrier strength improving with increasingly steep shear. This connection has also been corroborated by transport modeling assisted by gyro-fluid simulations. Rational safety-factor (q) values do not appear to play a role in the barrier formation, at least in the q range 1.3-2.3, as evidenced by the smooth dependence of the confinement enhancement on the loop voltage over a broad eITB database. MHD mode activity is however influenced by rational q values and results in a complex, sometimes cyclic, dynamical evolution.

1. Introduction

Electron internal transport barriers (eITBs) [1-2] have been obtained and studied in the TCV tokamak [3] (R=0.88 m, a=0.25 m, I_p<1 MA, B_ϕ<1.54 T, total ECRH power up to 4.5 MW) with strong electron cyclotron resonance heating (ECRH) in a variety of conditions. Fully non-inductive scenarios involve an appropriate distribution of current drive (ECCD) sources sustaining a hollow current profile, further enhanced by the bootstrap current centered in the high gradient barrier region [4-7]. Depending on the details of the discharge parameters and conditions, these scenarios may or may not evolve to a true steady state, whose duration is limited merely by equipment constraints and can equal several current redistribution times and up to hundreds of electron energy confinement times. Stationary eITBs are also observed in nearly noninductive conditions, with a small Ohmic current used to fine-tune the current profile [8], as well as in discharges with comparable Ohmic and noninductive current components [9]. Finally, transient eITBs have been generated in the absence of current drive, by strong heating during current ramps. All these scenarios display a significant improvement in confinement, quantified by an energy confinement time enhancement over TCV L-mode scaling (the Rebut-Lallia-Watkins scaling [10]), H_{RLW}, ranging from 3 to 6.

Although the various paths delineated above give rise to eITBs with widely varying characteristics, on average the highest performance discharges also display high bootstrap current fractions and high poloidal beta, as shown in Fig. 1 for a database of stationary eITBs. Higher enhancement factors have been reached in non-stationary conditions, and the bootstrap fraction has reached 90% transiently during early current ramps.

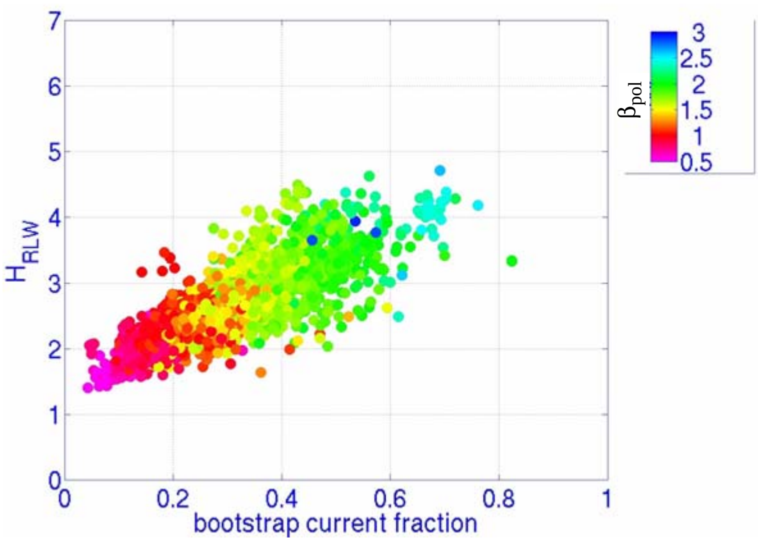

FIG. 1. Electron energy confinement enhancement factor over the Rebut-Lallia-Watkins scaling (TCV L-mode scaling) vs. bootstrap current fraction for a database of steady-state eITBs in TCV. The color coding refers to β_{pol}.

All the eITB scenarios achieved to date have relied for auxiliary heating solely on the second harmonic X-mode (X2) ECRH system, composed of six 82.7 GHz gyrotrons delivering 0.45 MW each to the plasma through independent real-time-steerable launchers. The operational recipes that have been established for generating eITBs depend on the accurate positioning ability of the launchers, as the properties and dynamic evolution of the discharge have been shown to be very sensitive to the heating locations and parallel wave numbers of the various beams [6,9,11]. The steerability of the launchers can then be employed to control the eITB performance in dynamically varying scenarios. This has been demonstrated in recent open-loop control experiments in which the flexible plasma position and shaping control system of TCV was used to move the plasma vertically (in order to increase the effective spatial resolution of Thomson scattering measurements), and the beam aiming was pre-programmed to track the plasma displacement, keeping the eITB confinement enhancement factor constant. The control case with the beams kept fixed, by contrast, resulted in a loss of confinement [6].

2. The role of the current density profile in eITBs

The plasma current profile clearly plays the dominant role in determining the conditions under which a barrier can occur and also in regulating its properties and dynamic evolution. This role has been established by several dedicated studies. Since TCV lacks a direct current density measurement at present, a combination of modeling and indirect experimental measurements is used to estimate the current profile. The Ohmic and bootstrap current densities can be derived from temperature and density measurements by Thomson scattering, and the EC-driven current density is calculated by the Fokker-Planck code CQL3D. The latter calculation is strongly dependent on the choice of the cross-field electron diffusivity, which in TCV regulates the ECCD broadening as well as the total driven current [12-14]. The primary constraint in the simulation is the imposition of the total EC-driven current, which is obtained by subtraction of the Ohmic and bootstrap components from the total current. The diffusivity is adjusted so that the simulated current obeys this constraint. To perform the calculation rigorously, the computed ECCD current profile is then fed into the transport code ASTRA [15], used in the so-called diagnostic mode, in which the pressure profile is fixed (and thus the Ohmic and bootstrap currents are too) and taken from experimental data: the code calculates the total current density profile and the plasma equilibrium self-consistently, ultimately generating the safety factor (*q*) profile [16]. The dominant uncertainty in the procedure is the value of the effective charge Z_{eff}, which is difficult to determine accurately and affects significantly both the Ohmic and ECCD current estimations.

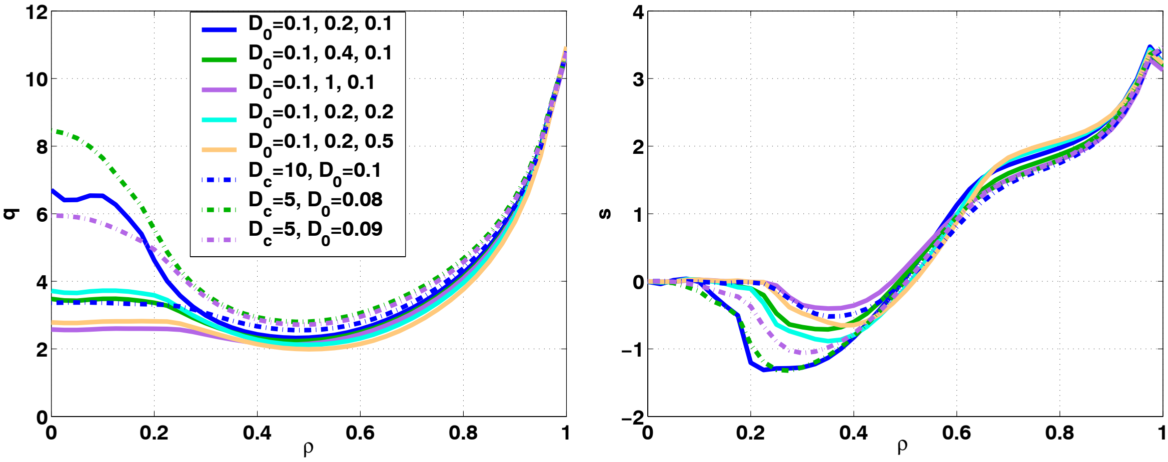

Fig. 2. (a) Safety factor and (b) magnetic shear profiles calculated by the ASTRA *transport code, used in diagnostic mode, for TCV discharge 28873 from ECCD calculations by* CQL3D *with different electron diffusivity profiles, constrained by the total driven current and by the electron temperature profile. Solid curves: piecewise uniform diffusivity (core, barrier, outside); dashed curves: diffusivity proportional to power-balance energy diffusivity, with varying core values. The radial coordinate here is the normalized square root of the poloidal flux.*

In steady-state, fully noninductive eITBs the problem is greatly simplified since the Ohmic current vanishes. These scenarios offer strong evidence that the current profile is non-monotonic [5], and indeed that the appearance of the barrier is tied both spatially and temporally to the appearance of a minimum in the *q* profile [4,7]. This correlation has also been corroborated by transport modeling [7].

The dependence of the reconstructed *q* profile on the details of the particle diffusivity used in CQL3D has recently been investigated [16]. Within the sole global constraint provided by the total driven current, there is considerable freedom in the choice of the radial diffusivity profile. Further constraints must be sought from other experimentally measured quantities. One plausible approach is to assume a proportionality between the particle diffusivity and the energy diffusivity inferred from power balance calculations. As the latter is poorly constrained in the immediate proximity of the magnetic axis, where little power is deposited, the core diffusivity remains a free parameter. An alternative approach has also been explored, involving a piecewise uniform diffusivity in the three well-defined regions corresponding to the barrier itself and to the spaces inside and outside it. As CQL3D simulations are performed by constraining the density profile to the experimentally measured one, the varying quantity is the electron temperature, and the free parameters must be adjusted to match its experimental profile. The *q* and shear [$s=(\rho/q)dq/d\rho$] profiles calculated for a fully noninductive discharge from a range of valid choices within the two approaches are shown in Fig. 2. The eITB in this case is located at $\rho=0.55\pm0.05$. The result demonstrates a remarkable resiliency of the *q* profile from well inside the barrier ($\rho=0.4$) out to the plasma edge, with a noticeable variance of the (negative) shear only in the inner core. While this variance can be significant in detailed comparisons with theory, the primary result - that the *q* profile is non-monotonic - is firmly supported by this sensitivity study.

The role of the current profile has been conclusively proven by an experiment exploiting the very large current drive efficiency of the Ohmic transformer to introduce small current perturbations accompanied by negligible energy transfer. Small increases or decreases in the central current density can dramatically degrade or enhance the confinement, respectively, while the location of the barrier is largely unaffected (Fig. 3) [8]. This experiment replicates in a more

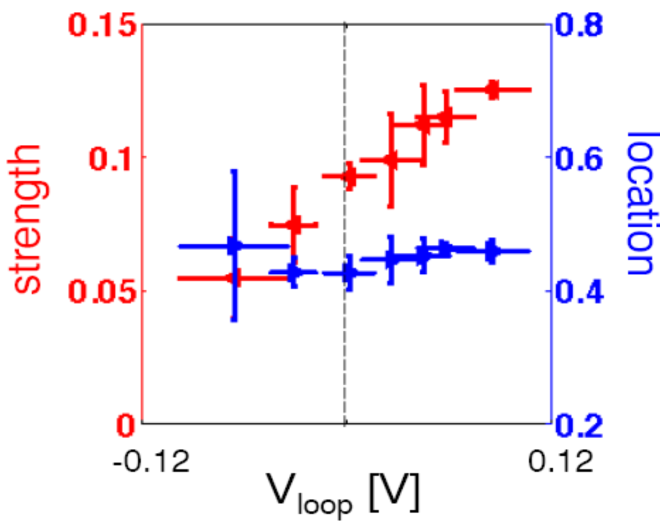

Fig. 3. Electron internal transport barrier strength (ρ_s, the ion sound gyroradius normalized to the electron temperature gradient scale length on the outer mid-plane) and location (radial coordinate equal to the normalised square root of the plasma volume) as functions of the surface loop voltage for a set of Ohmic current perturbation experiments in otherwise noninductive discharges. A negative voltage corresponds to a positive current.*

controlled fashion earlier studies performed with varying central ECCD components [9] and confirms that a negative central q shear is crucial to the creation of a barrier, with the barrier steepness and attendant confinement enhancement increasing with increasing central shear (in absolute value).

The Ohmic perturbation method, in addition, permits the observation of the transient effect of resistive current penetration into the plasma: as a positive current diffuses inward, and before it reaches the location of maximum current density, its effect is initially to deepen the central current hole, i.e. the negative central shear becomes even more negative; only when current diffusion is complete does the shear become less steep. The opposite is true in the case of negative current injection. This transient effect is predicted by ASTRA transport simulations and has the experimentally observed effect of causing an initial enhancement or degradation of the barrier (in the cases of positive or negative injection, respectively) before the effect is reversed, as shown in Fig. 4.

The smooth dependence of the confinement enhancement on the perturbative loop voltage, evidenced by Fig. 5, as well as the independence of the steady-state result on the history of this voltage (and thus on the safety factor profile evolution), strongly suggest that rational q values do not play a role in the formation of the barrier, at least in the range $1.3<q<2.3$ [6].

3. The properties and dynamics of eITBs

Barriers appear both in the electron temperature (T_e) and density (n_e) profiles (see Fig. 6). In the steady-state phase, the two barriers are strongly correlated in space and steepness, as they occur at the same location with the ratio $1/\eta_e$ of the logarithmic n_e gradient to the logarithmic T_e gradient approximately equal to 0.4-0.5 [17]. While no such correlation exists in L-mode discharges, in which $1/\eta_e$ varies with plasma conditions and heating characteristics, this

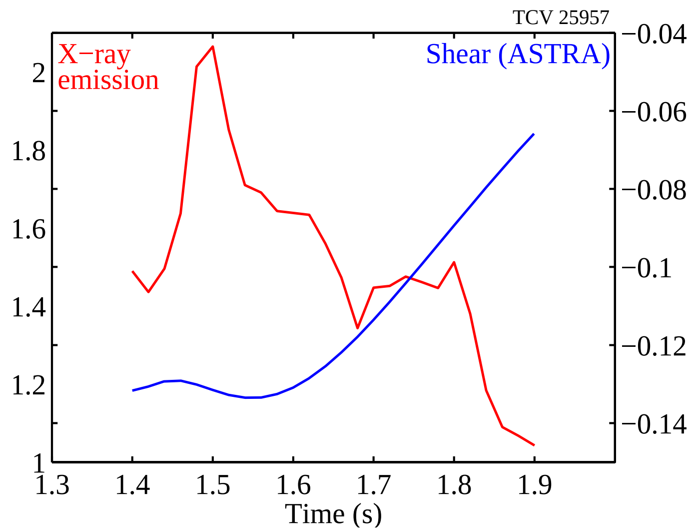

FIG. 4. X-ray emissivity and magnetic shear, as calculated by ASTRA, averaged in the negative-shear region. Noninductive discharge, 65 mV positive loop voltage applied externally from 1.4 s.

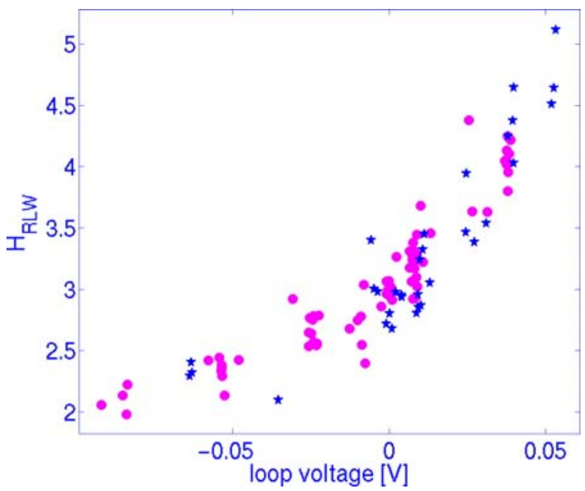

Fig. 5. Confinement-enhancement factor in the steady-state phase vs. loop voltage applied to an established eITB (blue) or before the barrier formation (magenta). A negative voltage corresponds to a positive current.

parameter takes the asymptotic value of 0.4-0.5 in all fully developed eITBs. In particular, starting from fully noninductive conditions, the further barrier enhancement by a negative Ohmic current perturbation [8], and the attendant change in the *q* profile, do not affect $1/\eta_e$ [17].

Under the conditions of these experiments, neoclassical transport would result in a value of $1/\eta_e$ close to the measured one [17]. This suggested the possibility that turbulence suppression may result in transport being reduced to neoclassical levels, and motivated an experimental campaign to measure particle transport directly in these scenarios, using pulsed gas injection. These studies have yielded values for the diffusivity and convection velocity of, respectively, 0.3 m^2/s and 1 m/s at the barrier location; while these values are 3 to 5 times lower than their L-mode counterparts, they still exceed neoclassical transport coefficients by an order of magnitude [18]. Neoclassical transport therefore remains negligible in these discharges.

The two primary effects of turbulence on particle transport are turbulent equipartion (TEP) [19] and anomalous thermodiffusion (THD) [20]. The former, while significant in strongly heated L-mode discharges, vanishes at zero magnetic shear and is proportional to the temperature gradient scale length, and thus becomes negligible in the case of a transport barrier with a reversed shear profile. The role of THD depends on the behavior of the dominant underlying instability, which for strongly EC-heated plasmas is the trapped electron mode (TEM). This mode is strongly stabilized inside the barrier, as a result of the negative magnetic shear, as shown by gyro-Landau fluid simulations with the GLF23 code [21] in Fig. 7. However, transport is still dominated by TEM-induced THD partly because the diffusion coefficient has a maximum at very low growth rates [18], and partly because of the concomitant quenching of TEP. The experimental value of $1/\eta_e$ is fairly closely reproduced by GLF23 simulations, except in the immediate neighborhood of the location of zero magnetic shear, where the density profile is incorrectly predicted to be flat (see Fig. 8). These simulations however ignore the parallel electron dynamics, i.e. the parallel wave number is set to zero. The inclusion of parallel dynamics in future modeling may conceivably resolve the remaining discrepancy.

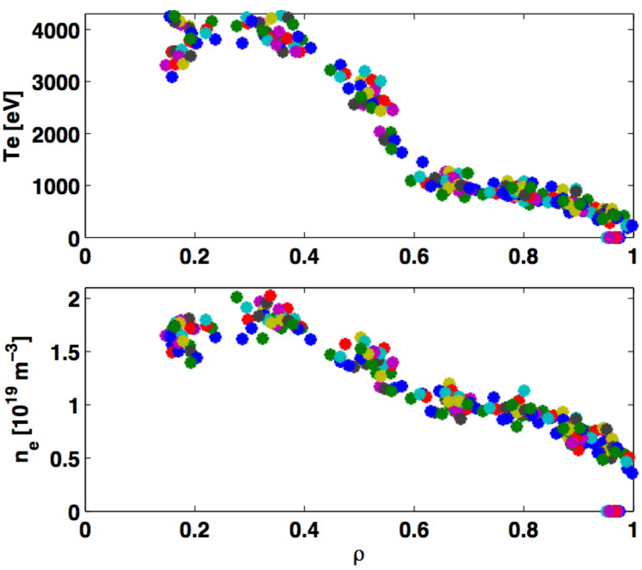

Fig. 6. Electron temperature (top) and density (bottom) profiles from pulsed Thomson scattering measurements, with spatial resolution enhanced by plasma position sweeping (tracked by the ECRH beams), for TCV discharge 29948.

The dynamical evolution of an eITB after the initial, rapid inception can be quite

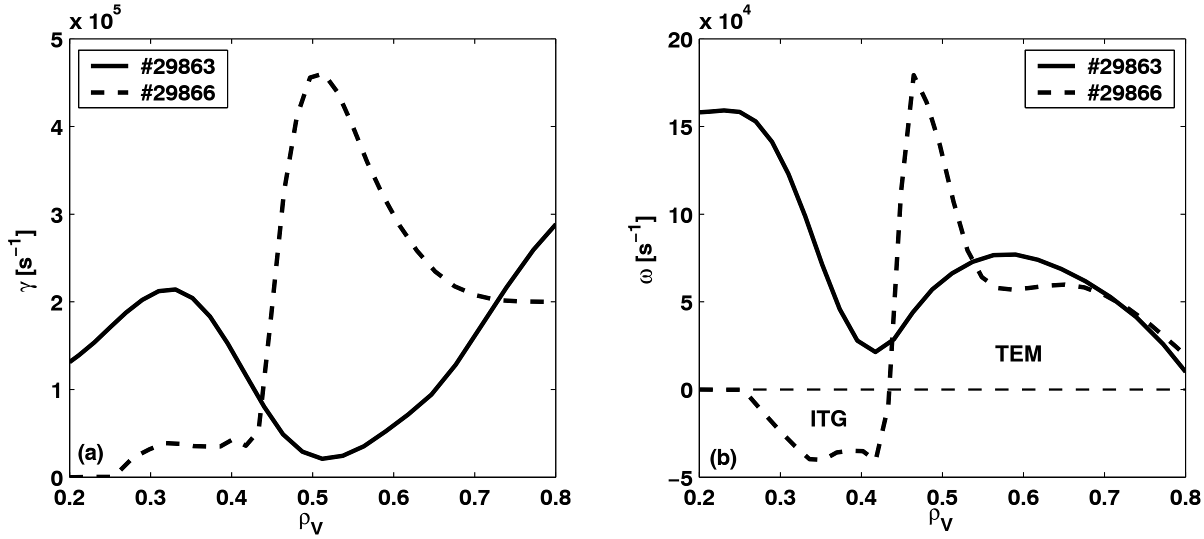

Fig. 7. (a) Growth rate and (b) real frequency of the most unstable mode, as calculated by GLF23, vs. minor radius for a monotonic-q, L-mode discharge (29863) and an eITB discharge (29866).

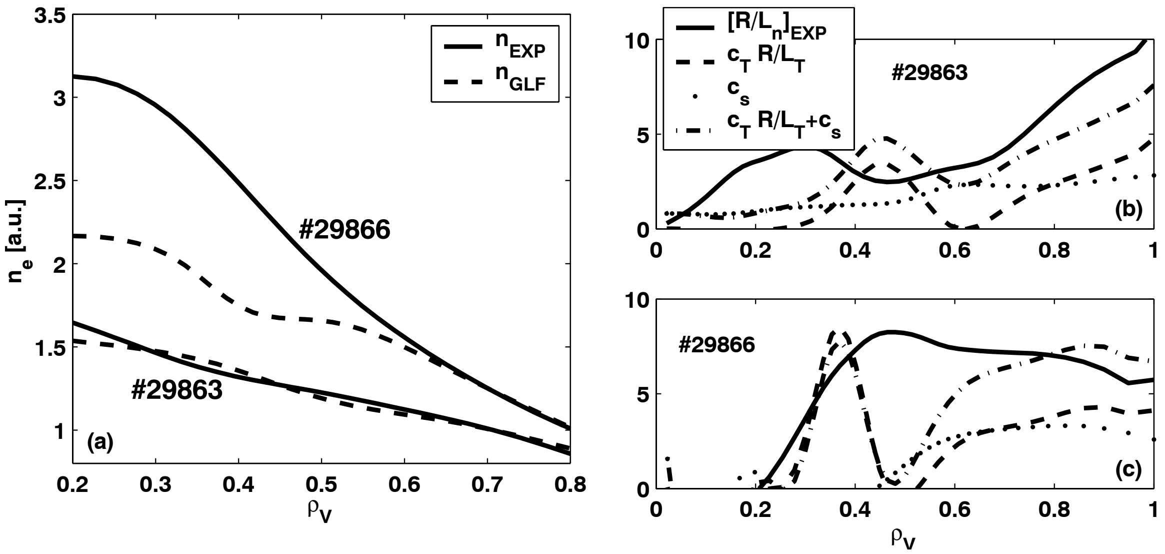

Fig. 8. (a) Experimental density profiles (solid curves) vs. profiles calculated by GLF23 (dashed curves) for the discharges of Fig. 7; (b-c) for the two discharges, experimental (solid curve) and calculated (dash-dotted curve) density gradient; the dashed and dotted curves are the TEP and THD contributions to the calculated gradient, respectively.

complex. In fully noninductive conditions with the barrier being generated by off-axis co-ECCD, a second, slower stage of barrier growth is often observed, after a delay of the order of the current redistribution time [6]. This effect is attributed to a feedback loop internal to the plasma, in which the key role is played by the bootstrap current. As the current profile relaxes after the barrier is initially formed, the relative locations of the barrier and of the heating sources can change slightly. As a result, more power can be deposited inside the high confinement region, resulting in a further increase in the gradients and thus in the bootstrap current, which is centered on the barrier and plays a dominant role in sustaining the hollow current profile. Being based on relative displacements that are even smaller than the very high aiming accuracy of the microwave beams, this feedback loop can also easily become negative, causing a deterioration of the barrier instead of an enhancement. A cyclic behavior has also been observed in some cases, with several barrier collapses and regenerations during a single discharge. This high sensitivity to power deposition results in a certain degree of variability between nominally identical scenarios. However, the robustness of the configuration is greatly increased when a significant amount of power is deposited deliberately well inside the barrier in order to exploit the high confinement and optimize the overall plasma performance [6].

4. MHD activity in eITBs

While rational *q* surfaces do not appear to play a role in the formation of eITBs, as discussed in section 2, the *q* profile does affect the MHD stability of the discharge, and strong internal modes develop in some cases which can significantly degrade the confinement [5].

Slow oscillations of the electron temperature have been recently investigated in eITB scenarios, both in noninductive and inductive conditions. Although these oscillations have very low frequency (~10 Hz) and are azimuthally and poloidally symmetric (m=n=0) and thus are not of an MHD nature themselves, they are seen to coexist with underlying MHD modes [22-23]. A similar phenomenon has been documented on the Tore Supra tokamak, where it has been dubbed O-regime and occurs in fully or nearly noninductive discharges with lower hybrid current drive and negative central magnetic shear [24].

An example is shown in Fig. 9 for a fully noninductive case. These oscillations affect the whole plasma column, as the total plasma current oscillates (with a 45^{o} phase shift with respect to the temperature oscillations) and the magnetic axis shifts radially by up to 3 cm. As shown in Fig. 9(c), an MHD mode is present and its amplitude oscillates 180^{o} out of phase with respect to the temperature. A feedback loop therefore appears to be at play, in which the MHD mode degrades the confinement, which in turn reduces the gradients and the MHD drive, so that a semi-stable oscillation can take hold. The bootstrap current fraction varies by 40-60%. The mode is found

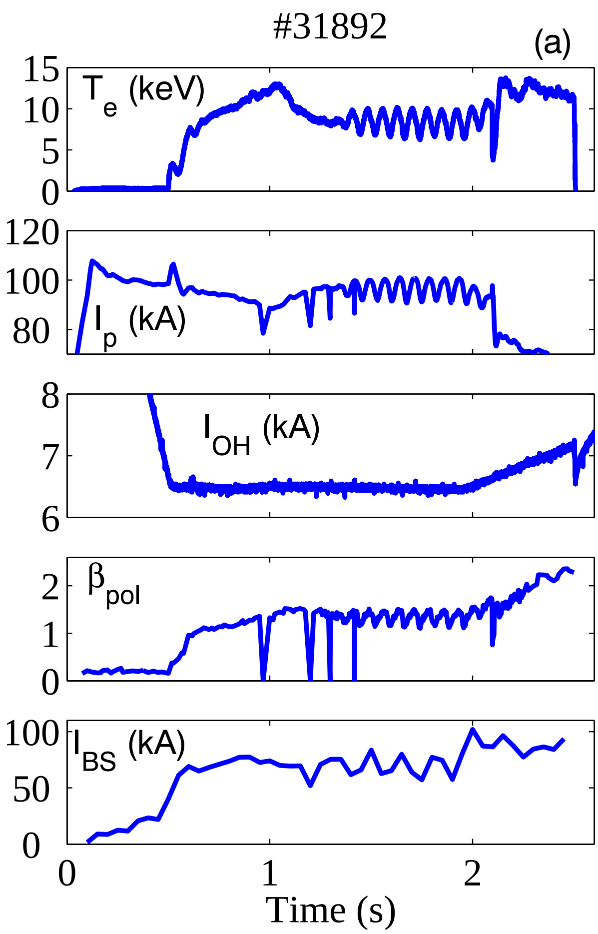

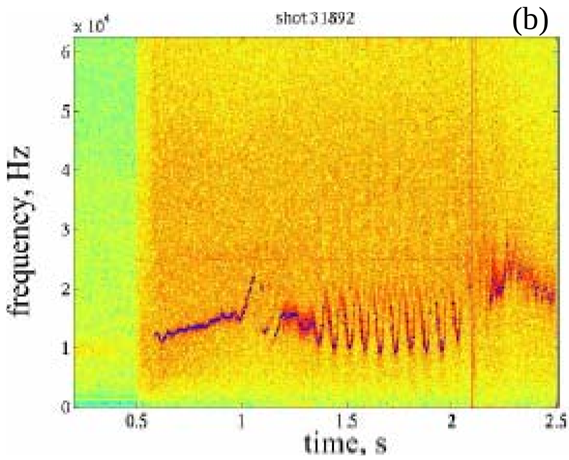

Fig. 9. (a) Electron temperature, plasma current, Ohmic transformer current, poloidal beta, bootstrap current; (b) spectrogram of magnetic probe signals.

to have helicity m/n=3/1 for the case of Fig. 9 [25], but a 2/1 mode has been found to be dominant in other cases. Studies employing the Ohmic current perturbation method are underway with the aim of exploring the conditions under which a stable cyclic behavior can occur, and particularly the dependence of this phenomenon on the details of the q profile and of the barrier characteristics.

Acknowledgments

We are grateful to the entire TCV team for the operation of the tokamak and of the auxiliary heating systems. This work was supported in part by the Swiss National Science Foundation.

References

[1] CONNOR, J.W., et al., Nucl. Fusion **44** (2004) R1.
[2] WOLF, R.C., Plasma Phys. Control. Fusion **45** (2003) R1.
[3] HOFMANN, F., et al., Plasma Phys. Control. Fusion **36** (1994) B277.
[4] HENDERSON, M.A., et al, Phys. Rev. Lett. **93** (2004) 215001.
[5] CODA, S., et al, Phys. Plasmas **12** (2005) 056124.
[6] GOODMAN, T.P., et al, Plasma Phys. Control. Fusion **47** (2005) B107.
[7] HENDERSON, M.A., et al, Nucl. Fusion **45** (2005) 1642.
[8] SAUTER, O., et al, Phys. Rev. Lett. **94** (2005) 105002.
[9] HENDERSON, M.A., et al, Plasma Phys. Control. Fusion **46** (2004) A275.
[10] REBUT, P.H., LALLIA, P.P., WATKINS, M.L., Plasma Phys. and Control. Fusion Research (Proc. 12th Int. Conf., Nice, 1988), IAEA, Vienna, 1989, Vol. 2, p. 191.
[11] HENDERSON, M., et al., Phys. Plasmas **10** (2003) 1796.
[12] HARVEY, R.W., et al., Phys. Rev. Lett. **88** (2002) 205001.
[13] NIKKOLA, P., et al., Nucl. Fusion **43** (2003) 1343.
[14] CODA, S., et al., Nucl. Fusion **43** (2003) 1361.
[15] PEREVERZEV, G.V., et al., Nucl. Fusion **32** (1992) 1023.
[16] ASP, E., et al., Theory of Fusion Plasmas (Proc. Joint Varenna-Lausanne Int. Workshop, 2006), Società Italiana di Fisica, Bologna, 2006, to be published.
[17] FABLE, E., et al., Plasma Phys. and Control. Fusion **48** (2006) 1271.
[18] FABLE, E., et al., Theory of Fusion Plasmas (Proc. Joint Varenna-Lausanne Int. Workshop, 2006), Società Italiana di Fisica, Bologna, 2006, to be published.
[19] BAKER, D.R., ROSENBLUTH, M.N., Phys. Plasmas **5** (1998) 2936.
[20] MISKANE, F., GARBET, X., Phys. Plasmas **7** (2000) 4197.
[21] WALTZ, R.E., et al., Phys. Plasmas **4** (1997) 2482.
[22] UDINTSEV, V.S., et al., Control. Fusion and Plasma Phys. (Proc. 33rd EPS Conf., Rome, 2006), D1.003, to be published in Europhys. Conf. Abstr. (2006).
[23] UDINTSEV, V.S., et al., submitted to Fusion Sci. Technol. (2006).
[24] GIRUZZI, G., et al., Phys. Rev. Lett. **91** (2003) 135001.
[25] TURRI, G.P., et al., Control. Fusion and Plasma Phys. (Proc. 33rd EPS Conf., Rome, 2006), P1.148, to be published in Europhys. Conf. Abstr. (2006).